Linking a One-Dimensional Reverberation Chamber Model with Real Reverberation Chambers

(Article begins on next page)

28 April 2024

Linking a One-Dimensional Reverberation Chamber Model with Real Reverberation Chambers

Ramiro Serra and Flavio Canavero

Politecnico di Torino, Dipartimento di Elettronica, EMC Group
Torino, Italy, Email: {ramiro.serra, flavio.canavero}@polito.it

Abstract—Our work focuses on the study of a simple yet complete one-dimensional reverberation chamber model presented previously. The statistical properties of the fields are introduced either by varying the width or the relative dielectric constant of a perturbing lossless layer. Our aim is to show the excellent agreement between this simple model and real RCs. The field statistics in *undermoded* regime is examined. An intuitive three-dimensional extension of the model is presented as a rectangular non-homogenous cavity. With the use of a suitable change of variables, we are able to find an analogous RC model which results in an homogeneously-filled cavity, with a geometrical discontinuity mainly consisting of a conducting box inside the cavity. The final result is to link the one-dimensional virtual stirrer with a real one. This process is performed provided we can calculate (even numerically) the monostatic radar cross section of the actual rotating stirrer under study. Excellent agreement with measurements were found.

I. INTRODUCTION

Reverberation Chambers (RC) are gaining significant confidence in their use for radiated emissions and immunity measurements. RC users need to fully understand its working principles in order to correctly interpret the measurement results and to optimize the performance for various measurement tasks.

RCs' extensive knowledge up to now, result from a partial juxtaposition of four different approaches: the deterministic models, the statistical models, the empirical techniques and the computer/numerical methods. It is not possible to leave one of this approaches behind, as each one of them behaves as a non-exhaustive, non-excluding part of RC description. Furthermore, they mutually collaborate to give fairly successful answers in fields where the other one fails, and viceversa. Therefore, there is an obvious gap which makes us change our methodology depending on what kind of result we seek. In this sense it is to point out that a statistical description is meaningful only if the chamber is working in an *overmoded* regime and only on special chamber geometries (for example, the Plane Wave Integral Representation [1] has its rigorous validity only in spherical volumes). On the other hand, the deterministic models' success is intimately linked to the specificity of

the chamber geometry, but it is decoupled from the mode stirring process, which is an essential constituent of the RC performance. Consequently, a call for filling this gap and linking the two approximations is needed. This necessity is supported by the aim of having a better understanding, to manage a simpler yet complete model and to reduce up to a reasonable minimum the empirical techniques.

An attempt of filling this gap was presented in [2], where a one-dimensional RC model (see figure 1 for a schematic diagram) was shown to have a statistical behavior equal to real RCs. The statistically uniform field can be obtained by means of different stirring processes such as, i.e. varying the size $t = x_2 - x_1$ and/or the relative dielectric constant κ of a 1D "stirrer" (a perturbing lossless dielectric layer) placed inside a theoretical vacuum-filled 1D segment.
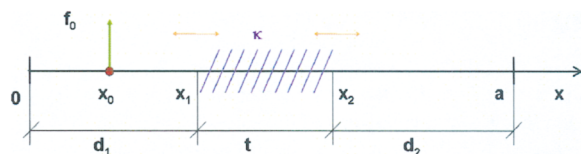

Figure 1. Definition of the one-dimensional cavity under study.

Section II will extend this 1D RC model to an *undermoded* regime. In section III a three-dimensional extension of this model will be presented and its analogous homogeneously-filled non-rectangular RC model, found by means of a suitable change of variables. Section IV will present some test cases in order to validate the performance of this model.

II. UNDERMODED REGIME

One of the essential conditions for the correct functioning of Reverberation Chambers is that it has to work under an *overmoded* situation. Unfortunately, the question about when does a chamber exactly starts to be in an *overmoded* regime remains unanswered (only rule-of-thumb techniques are provided to estimate it, as in [3]).

Although comparatively little work has been reported on *undermoded* RCs, this subject is of a great practical in-

terest. Low-frequency operation, i.e. near the lowest usable frequency (LUF) of the chamber, often means consistent deviations from ideal field distributions. An accurate estimate of the theoretical distribution function at low frequency can help RC users to optimize the band of operation within a given chamber size.

We will demonstrate in the following, that our 1D RC model can reproduce the main literature findings in this area.

A. Effect of the Number of Modes on the Field Statistics

From what has been reported (i.e. [1], [4]) and empirically found in measurements, *nonnormal* data distributions correspond to a chamber with a relatively low number of modes present (i.e. *undermoded* case) and, on the other hand, *normal* data distributions correspond to a chamber with a relatively high number of modes present (i.e. *overmoded* case).

In the one-dimensional case, it is very straightforward to find out the total number of modes N excited inside the cavity without the stirrer as a function of the source frequency f_0. It is:

$$N = \left\lfloor \frac{2a}{c_0} f_0 \right\rfloor \tag{1}$$

where a is the cavity length and c_0 the speed of light.

To start our analysis, four different values of N were selected to calculate the RC response. The number of modes were chosen to be $N = 10$, $N = 15$ (two *undermoded* situations), $N = 20$ and $N = 100$.

The resulting field distributions of the real part of the electric field are compared in Figure 2. It could be seen a tendency to normality as the total number of modes increases, but using only a qualitative assessment these differences seem close to be negligible.
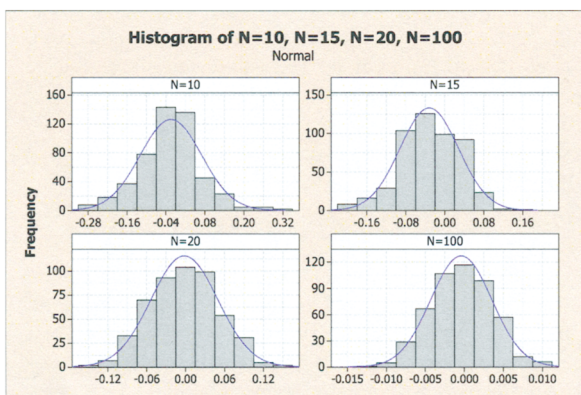

Figure 2.   Histograms of the real part of the electric field for a one-dimensional reverberation chamber when different number of modes are excited.

We will quantitatively assess these data with an Anderson-Darling (A-D) Normality Test [5]. Both situations when $N = 10$, $N = 15$ showed p-values below 0.005 while the other two sets of data show p-values of 0.435 and 0.769, thus largely justifying the hypothesis of normality.

This calculation seems to suggest that in this particular case, the step from the *undermoded* to the *overmoded* situation occurs at some point between $N = 15...20$ modes. The significative difference in the number of modes sufficient to reach the *overmoded* situation in this case with respect to the accepted in [3] (viz. $N = 60...100$) is not new, as reported i.e. in [6].

It is seen that the overall effect of the number of modes over the field statistics is in agreement with what is found in measurements.

B. Undermoded *Statistics*

Important contributions on this subject are found in [7] (and references therein), where theoretical first-order probability density functions are derived for the electromagnetic fields inside RCs. It basically uses the deviations of some physical characteristics of the fields in *undermoded* RCs, from those for ideal reverberation. In [8] the Weibull distribution is proposed to model the distribution of the magnitude of the electric field component.

The overall behavior of the fields described by these models is mainly to vary from χ_6^2 and χ_2^2 (i.e. exponential) distributions as the frequency of operation approaches the LUF. It is known that the Weibull distribution is a two-parameter distribution, with a shape parameter k and a scale parameter λ [9].

Figure 3 shows the histograms of the absolute value of the electric field with their fitted Weibull Distributions, calculated at a fixed measurement position inside the test volume after 500 independent calculations as explained in [2]. The six panels of figure 3 correspond to $F_3 = a/\lambda = 5, 10, 15, 50, 100, 200$ (F_3 is defined in [2], and λ refers to the wavelength of the source $\lambda = c/f_0$, not to the scale parameter of the Weibull distribution). Of the values chosen for F_3, three refer to an *undermoded* regime and three to an *overmoded* one.

It can qualitatively be seen that the Weibull distribution gives a very good and smooth approximation of the *undermoded*-to-*overmoded* regimes transition. Figure 4 shows the shape parameters k for values of $F_3 = a/\lambda$ ranging from 2 up to 100. It can be seen that the overall behavior is to converge towards a Rayleigh distribution ($k = 2$) from the exponential one ($k = 1$). This is mainly due to the capacity of the Weibull distribution of embody the asymptotic laws and to shift from an exponential distribution to a Rayleigh one. To make it easier to see, a fitted polynomial line was added to the curve.

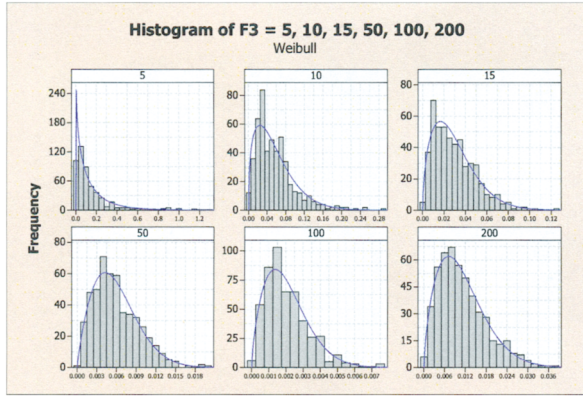All of the above is in excellent correspondence of what

Figure 3. Histograms of the absolute value of the electric field with their fitted Weibull distributions at a fixed measurement position inside the test volume for three undermoded and three overmoded regimes.
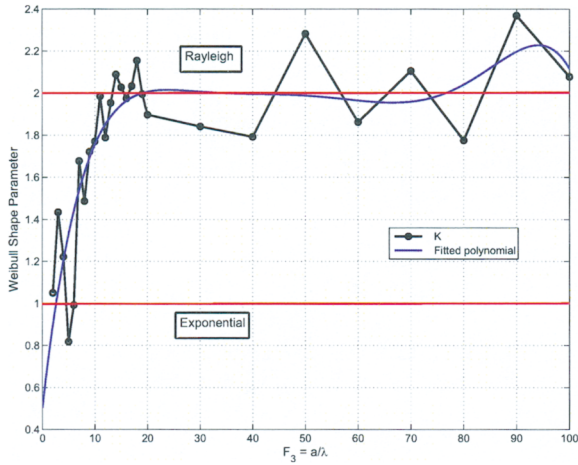

Figure 4. k shape parameter of the Weibull distribution fitting the data calculated from 500 independent variations of the stirrer.

is reported in [7] and [8].

C. Validity of the Physical Analogy of the Dielectric Stirrer

At this point, a question could arise: what is the link and correlation between real stirrers and our virtual "dielectric" stirrer?

The effect of placing a material with a considerable dielectric constant inside an electric field as in our cavity is mainly to change the configuration of the eigenvalues. It is analogous to adding a capacitance to a circuit, or a reactive load into a transmission line. As we are assuming that no losses are into the dielectric, what happens is that this new material inserted has stored some energy from the system. This would result in a particular field configuration. It is then intuitively easy to imagine that a little change in

size or in its relative dielectric constant, could generate a fairly different distribution of the field. The present analogy could be justified by the fact that usually, "complex-shaped" stirrers outperforms simpler ones (i.e., see [10], [11]).

Nevertheless, it is true that real stirrers do not "store" energy and so the problem remains unanswered in a closed manner. A change of variable strategy over a 3D extension of this model will be presented in the next section to solve this problem.

III.   3D EXTENSION

A change of variables will be applied to an extended 3D version of our 1D model, resulting in a successful strategy for its study. This process will help us identify one irregularly-shaped homogeneously-filled cavity, that resembles quite much the setup of a real RC.

A. The 1D Model Extended into 3D

The analogous 3D model of figure 1 is schematically shown in figure 5. In this non homogenously-filled cavity, the "dielectric" stirrer has width t, relative dielectric constant κ and its height and depth are equal to the cavity.
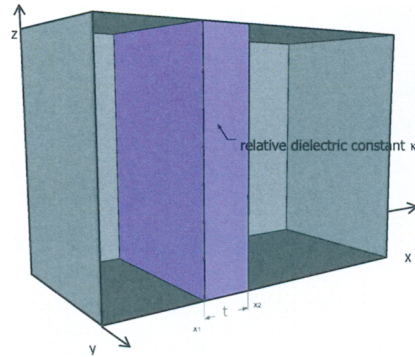

Figure 5. Cross section plane for the schematic figure of the three-dimensional cavity under study.

The electromagnetic field inside this chamber obeys the wave equation:

$$\nabla^2 \vec{E}(\vec{r}) + \kappa(\vec{r})k^2\vec{E}(\vec{r}) = \delta(|\vec{r} - \vec{r_0}|), \qquad (2)$$

where

$$\kappa(\vec{r}) = \begin{cases} \kappa & x_1 \leq x < x_2 \\ 1 & elsewhere \end{cases}$$

and $k = \omega\sqrt{\mu\epsilon}$ is the free-space wavenumber; μ, ϵ are the free-space permeability and permittivity, respectively, $\vec{r}$ is the position vector in cartesian coordinates and $\vec{r_0}$ the position of the point source. The $e^{-j\omega t}$ time dependence is suppressed.

B. Change of Variables Basic Theory

Let us consider the inhomogeneous Helmholtz equation in three dimensions:

$$\left[\nabla^2_{xyz} + k^2\right] f(x,y,z) = g(x,y,z).\qquad(3)$$

Let us apply the function $f : \mathbb{R}^3 \to \mathbb{R}^3$ with components:

$$u = f_1(x,y,z)$$
$$v = f_2(x,y,z)$$
$$w = f_3(x,y,z),$$

to (3) to obtain a slightly more complicated equation

$$\left[\nabla^2_{uvw} + k^2/J_{uvwxyz}\right] F(u,v,w) = G(u,v,w),\qquad(4)$$

where $\nabla^2_{uvw} = \partial^2/\partial u^2 + \partial^2/\partial v^2 + \partial^2/\partial w^2$ and J_{uvwxyz} is the Jacobian determinant of the transformation $(x,y,z) \leftrightarrow (u,v,w)$ associated with the change of variables

$$J_{uvwxyz} = \begin{vmatrix} \partial u/\partial x & \partial u/\partial y & \partial u/\partial z \\ \partial v/\partial x & \partial v/\partial y & \partial v/\partial z \\ \partial w/\partial x & \partial w/\partial y & \partial w/\partial z \end{vmatrix}.\qquad(5)$$

Equation 4 corresponds to an inhomogeneous medium situation, where the wavenumber k would be a function of the coordinates.

C. Changing Domains

The cavity described in Section III-A is indeed of the same class of (4) if we assume that $\kappa(u,v,w) = 1/J_{uvwxyz}$. Let us now suppose it as if it were a certain cavity in the transformed domain and find out a geometry in the physical domain that maps into it. In other words, we would like to find out a change of variables $f : \mathbb{R}^3 \to \mathbb{R}^3$ whose Jacobian determinant corresponds to the inverse of the $\kappa(u,v,w)$ function. One possible solution was found to use the following transformation

$$\begin{aligned} u &= x \\ v &= y \\ w &= \begin{cases} z & 0 \le x < x_1 \\ z/\kappa + g(y) & x_1 \le x < x_2 \\ z & x_2 \le x \le a \end{cases} \end{aligned}\qquad(6)$$

in the cavity depicted in figure 6, where

$$g(y) = c\left(1 - \frac{1}{\kappa}\right)(H(y-y_1) - H(y-y_2) + 1),\qquad(7)$$

and $H(y)$ is the Heaviside step function.

It is quite straightforward to see that the change of variables in (6) will have a Jacobian determinant as the one we search for.
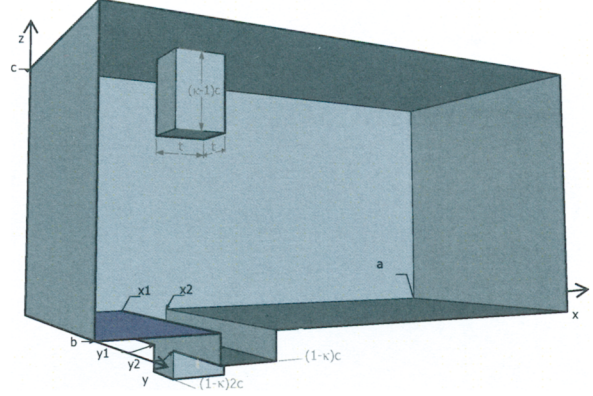

Figure 6. Cavity of figure 5 in the assumed physical domain.

D. Highlighting the Analogy

The cavity geometry conceived as our new physical domain has two discontinuities in the horizontal walls of the cavity: a "box" of height $(\kappa - 1)c$ and square section of side $t = x_2 - x_1 = y_2 - y_1$ pending from the roof, and an "inverted podium-like" discontinuity in the floor.

The discontinuities are a function of κ. In fact, if we make $\kappa = 1$ in the physical domain, this means that no discontinuity steps are present. On the transformed domain, this means that the perturbing layer is made of vacuum. So the change of variables will transform a rectangular cavity into itself.

We have then establish an homogeneously-filled non-rectangular cavity that is analogous to another rectangular non-homogeneous cavity which is a 3D extension of our 1D RC model of figure 1. The mode-stirring process in the 1D RC model was obtained by varying the dielectric layer width t and/or its relative dielectric constant κ. It is reasonably expectable that the 3D model with the dielectric slab would work in the same way, and so, its analogous cavity.

The analogy stands that a variation in the width t of the dielectric is equivalent to a variation of the width and depth of the metal box and a variation of the relative dielectric constant κ is equivalent to a variation in the metal box height. Also the podium-like discontinuity will change its aspect as a function of t and κ.

E. Linking the Model

If we concentrate only in the upper discontinuity, we can see that the mode stirring process inside this RC model is due to a metallic box that is changing its height and section. This description is quite close to real RCs, if we think that the shape-changing metal box is acting similar to a rotating stirrer. In order to relate the effect of them (the box and an actual stirrer) on RCs statistical behavior, a Radar Cross

Section (RCS)-based calculation in *free space* with plane wave illumination will be applied.

The RCS σ is the measure of a target ability to reflect radar signals in the direction of the radar receiver, i.e. it is a measure of the ratio of backscatter power per unit solid angle in the direction of the incident wave (from the target) to the power density that is intercepted by the target. Mathematically the RCS can be represented as

$$\sigma = 4\pi \frac{P_{backscatter}}{P_{intercepted}} \quad (8)$$

The idea is to generate a changing in the dimensions of the front panel of the metal box whose RCS is able to follow that of the rotating stirrer. The process is:

1) Calculate (or simulate numerically) the monostatic RCS of a stirrer in *free space* as a function of its rotating angle, $\sigma(\phi)$.
2) The relative dielectric constant is calculated from the relation of the stirrer height with respect to the height of the chamber in which it is inserted. Mathematically:

$$\frac{h_{metal\,box}}{h_{RC\,Model}} = \frac{h_{stirrer}}{h_{real\,RC}} \quad \Rightarrow \quad \kappa = \frac{h_{stirrer}}{h_{real\,RC}} + 1 \quad (9)$$

3) The layer width t is calculated knowing that the RCS of a planar surface $\tilde{\sigma}$ is

$$\tilde{\sigma} = 4\pi \frac{A^2}{\lambda^2} \quad (10)$$

where $A = (\kappa - 1)ct$ is the area of the front panel of the metal box.

4) Make $\tilde{\sigma} = \sigma(\phi)$ in order to get the variation of t as a function of the rotating angle, i.e. $t(\phi)$ as:

$$t(\phi) = \frac{\lambda}{2c(\kappa - 1)} \sqrt{\frac{\sigma(\phi)}{\pi}} \quad (11)$$

The 1D cavity length is chosen in a way that the same number of modes are present for a given frequency. Using the well-known formula in [3] for the number of modes inside a chamber and equation 1 we are able to deduce:

$$a = \frac{4\pi}{3} whl \frac{f^2}{c_0^2} - \frac{(w + h + l)}{2} + \frac{c_0}{4f}. \quad (12)$$

By this process we can run a simple experiment in a 1D RC model, which is able to reproduce the same statistical behavior of a particular stirrer inside a particular chamber.

IV. VALIDATION

In order to validate the previous considerations, an evaluation of the stirrers and chambers presented in [12] will be done. The choice of this set of experiments is mainly

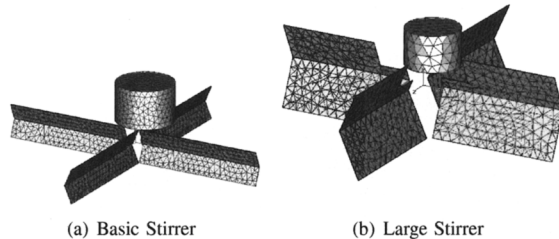(a) Basic Stirrer   (b) Large Stirrer

Figure 7. Stirrer models used in the measurements performed in [12].

due to the fact that every design parameter is provided in the report, so the link from real stirrers and RCs to the 1D model can be directly done.

A. Measurement Setup

In [12], stirrer efficiency measurements have been performed in FOA's RC facility that consists of two RCs (one large, E_3 and one smaller, E_4) of different size. Measurements were made with two different stirrers, named "basic stirrer" and "large stirrer", with 200 angular positions in the frequency range of 0.2 − 18 GHz. Figures 7(a) and 7(b) shows the stirrers models used to simulate their RCS.

The quantity used for the evaluation is the linear correlation coefficient [3]:

$$\rho(r) = \frac{1}{N - 1} \frac{\sum_{i=1}^{N} (x_i - \langle x \rangle) \cdot (x_{i+r} - \langle x \rangle)}{\sigma_x^2} \quad (13)$$

where N is the total number of stirrer positions and $x_1, x_2, x_3, \ldots$ is the normalized received power at consecutive stirrer positions. The subindex $i + r$ is *modulo N*.

B. Results

The RCS of the stirrers in figure 7 was simulated using the CST® simulation software. All the process explained in section III-E was applied in order to solve three different 1D models. Correlation coefficients for the two stirrers in different chambers are shown in figure 8. It can be seen that they have an excellent matching with the measurements reported in [12].

In figure 9 it can be seen that the correlation coefficient, when using the Basic Stirrer in RC E_3 is falling with respect to the frequency and increasing stirrer interval. This is in accordance of what reported in [12].

Many figures can be reproduced and they have all found the same correspondence with measurements. We omit them here for the sake of brevity.

(a) Basic Stirrer in E_3

(b) Basic Stirrer in E_4
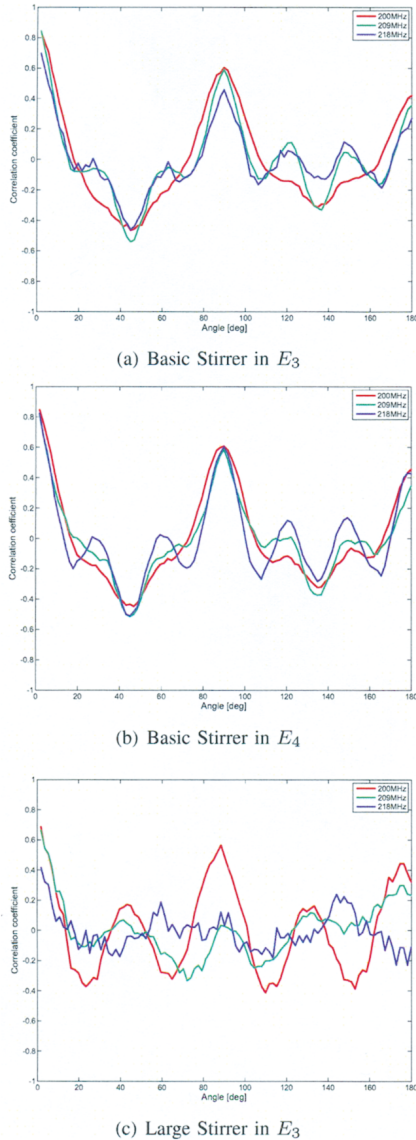

(c) Large Stirrer in E_3

Figure 8. Correlation coefficient for 3 frequencies vs. angular stirrer increment of the Basic and Large stirrer efficiency measurements performed in [12].
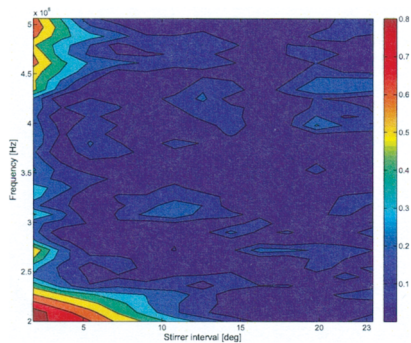

Figure 9. Correlation coefficient $|\rho|$ of the basic stirrer in RC E_3.

V. CONCLUSIONS.

This paper discusses the field statistics within a 1D RC model that presents a strong behavioral analogy with 3D RCs. Besides recognizing in it the same statistical behavior (as done in [2]), a further characteristic of real RCs was compared with our 1D RC model i.e. the field distribution in RCs working in *undermoded* regime and their statistics (section II). A 3D RC model was conceived as an intuitive extension of the 1D RC model presented. With the use of a proper change of variables, we can interpret the role of the dielectric stirrer as a geometrical discontinuity. Changing the width of the dielectric slab is equivalent to changing the width and depth of a "metal box" inside a cavity. Changing the relative dielectric constant is equivalent to changing the height of the "metal box". Knowing the monostatic RCS in *free space* of a particular stirrer, we are able to reproduce the same statistical behavior by means of linking the real setup with its 1D parameters. A validation analysis was done, confronting the mentioned process with real measurements reported in [12]. An excellent agreement was found. The main convenience of the 1D RC model consists on giving a complete understanding of RCs, without leaving any gap on its theoretical development. Future work (currently under way) involves a wider measurement campaign in order to better establish the correct analogy and convenience of this model.

REFERENCES

[1] D. Hill: "Plane Wave Integral Representation for Fields in Reverberation Chambers", *IEEE Transactions on EMC*,vol. 40,1998,pp. 209-217.

[2] R. Serra, F. Canavero: "A One-Dimensional Interpretation of the Statistical Behavior of Reverberation Chambers", *International Conference on Electromagnetics in Advanced Applications*, 2007, pp. 221-224.

[3] CISPR/A and IEC SC 77B: *IEC 61000-4-21 Electromagnetic Compatibility (EMC) - Part 4-21: Testing and Measurement Techniques - Reverberation Chamber Test Methods*, International Electrotechnical Commission (IEC) International standard, Aug. 2003.

[4] J. G. Kostas and B. Boverie: "Statistical model for a mode-stirred chamber", *IEEE Trans. Electromagn. Compat.*, vol. 33, pp. 366-370, 1991.

[5] L. C. Wolstenholme: *Reliability Modelling: A Statistical Approach*, CRC Press, London, 1999.

[6] M. O. Hatfield, M. B. Slocum, E. A. Godfrey, and G. J. Freyer: "Investigations to extend the lower frequency limit of reverberation chambers, in *Proc. 1998 IEEE Symp. Electromagnetic Compatibility*, Denver, CO, Aug. 2428, 1998, pp. 2023.

[7] L. Arnaut: "Compound Exponential Distributions for Undermoded Reverberation Chambers", *IEEE Transactions on Electromagnetic Compatibility*, Vol. 44, No. 3, August 2002.

[8] G. Orjubin, E. Richalot, S. Mengu, O. Picon: "Statistical Model of an Undermoded Revreberation Chamber", *IEEE Transactions on Electromagnetic Compatibility*, Vol. 48, No. 1, Febreuary 2006.

[9] A. Papoulis: *Probability, Random Variables, and Stochastic Processes*, New York: McGraw-Hill, 1965.

[10] C. Bruns, "Three-dimensional simulation and experimental verification of a Reverberation Chamber", PhD Thesis, Swiss Federal Institute of Technology, 2005.

[11] J. Clegg, A. C. Marvin, J. F. Dawson, S. J. Porter: "Optimization of stirrer design in a reverberation chamber", *IEEE Trans. on EMC*, November 2005.

[12] O. Lundén, L. Jansson, M. Bäckström: "Measurements of stirrer efficiency in mode-stirred reverberation chambers", FOA Technical Report: FOA-R–99-01139-612–SE, May 1999, Linköping, Sweden.